Far East Journal of Applied Mathematics
Volume 49, Number 2, 2010, Pages 85-106
Published Online: February 9, 2011
This paper is available online at http://pphmj.com/journals/fjam.htm

ON NONLINEAR bi-CHROMATIC WAVE GROUP DISTORTIONS

MASHURI[a,b], L. SHE LIAM[d], ANDONOWATI[a,c] and NINING SARI NINGSIH[e]

[a]Industrial and Financial Mathematic Research Division
Faculty of Mathematics and Natural Science
Institut Teknologi Bandung
Jl. Ganesa 10 Bandung 40132, Indonesia

[b]Department of Mathematics
University of Jenderal Soedirman
Jl. Dr.Soeparno 60 Karangwangkal
Purwokerto, Indonesia
e-mail: mas_huri@students.itb.ac.id

[c]LabMath Indonesia
Jl. Dago Giri 99, Warung Caringin
Bandung 40391, Indonesia
e-mail: andonowati@labmath-indonesia.org

[d]Department of Mathematics
University of Twente
P.O.Box 217,7500 AE Enschede, The Netherlands
e-mail: liesl@ewi.utwente.nl

[e]Department of Oceanography
Institut Teknologi Bandung
Jl. Ganesa 10 Bandung 40132, Indonesia
e-mail: nining@fitb.itb.ac.id

2010 Mathematics Subject Classification: 34E05, 74J30, 76B15.

Keywords and phrases: Non-Linear bi-chromatic wave, AB equation, KdV equation, third order expansion method

Received June 18, 2010

Abstract

A bi-chromatic signal that is subject to the Benjamin-Feir instability will show large deformations while propagates away from its source. For applications in hydrodynamic laboratories to generate large waves to test ships in extreme conditions, it is desired to know the location and height of the maximal waves with respect to the properties at the wave maker. In this paper we will show two different ways how to calculate both the location as well as the maximal wave high. First we show the AB-equation, an improved KdV-type of equation, can simulate numerically the experiments very accurately. Using a third-order expansion method for the AB solutions, we then show that the location of the largest deformation and the amplitude amplification due to nonlinear effects can well be calculated rather explicitly. This improves previous results using the third order approximation with a KdV equation, since the AB equation includes accurately second order non-linear terms that account also for the important third order nonlinear resonant wave interactions.

1. Introduction

At the current state much research related to accurately generating waves in hydrodynamic laboratories is being done. Studying wave propagation in well-controlled hydrodynamic laboratories is an interesting subject for practical purposes as well as for understanding properties of wave propagation itself. The motivation of this paper arises from the requirement of hydrodynamic laboratories to generate 'extreme waves' that do not break while running downward in the wave tank. Of particular interest is the accurate description of the non-linear wave deformations when traveling away from its generation point (the waveflap in laboratories). Large deformations were observed experimentally for bi-chromatic signals experiencing the Benjamin-Feir instability [6, 7]. Previous research showed that by using the improved KdV equation-the classical KdV but with exact linear dispersion-the position of the largest deformation can be predicted rather accurately with 3rd-order expansions. This model, however, fails to determine the correct amplitude amplification [5].

In this paper we will use a new KdV- type of equation, called the AB equation, to study the wave propagation. The equation is exact up to 2nd-order, i.e. it has exact linear dispersive properties and quadratic terms that include correct dispersion; see [3, 4]. This equation, unlike other KdV equations, can describe waves in infinitely deep water, but in this paper we only consider waves on finite depth.

We use this AB equation to simulate numerically the deformations and show that the results are remarkably good agreement with experiments. Besides that, analytical solutions will be constructed by using 3th-order asymptotic expansion. These approximations for AB will be compared to the approximates using the KdV equation as in [5]. To predict the position of maximal amplitude we use the concept of Maximal Temporal Amplitude (MTA), which measures the maximal height of the wave at all downstream positions.

The content of the rest of the paper is as follows. In section 2 we briefly describe the model equations mentioned above. In section 3 we describe concisely the 3th-order asymptotic method for the AB equation and compare the coefficients of the solution when using AB with those when using the KdV. In Section 4 we discuss the comparison between the bi-chromatic evolution of AB and KdV equation. Initially, the numerical simulation of AB is verified with experiment using MARIN data. Base on the numerical simulation, comparison between the bi-chromatic evolution using 3th-order asymptotic method for the AB and KdV and also MTA of AB and KdV will be presented. In Section 5 we give some concluding remarks.

2. Mathematical Model Equations

The wave equation used in [5] to determine the position of maximal amplitude and amplitude amplification factor is KdV-equation with exact linear dispersion but with classical nonlinearity. In physical variables it is given for the wave elevation η by

$$\partial_t \eta + i\Omega(-i\partial_x)\eta + c_0 \frac{3}{4h}\partial_x \eta^2 = 0; \tag{1}$$

here Ω is the pseudo-differential operator with $\Omega(k) = k\sqrt{g \tanh(kh)/k}$, $c_0 = \sqrt{gh}$, g is the gravitational acceleration and h is the depth of the layer. The AB-equation as derived in [3] reads

$$\partial_t \eta = -\sqrt{g} A\left[\eta + \frac{1}{2}A(\eta A\eta) - \frac{1}{4}(A\eta)^2 + \frac{1}{2}B(\eta B\eta) + \frac{1}{4}(B\eta)^2\right], \tag{2}$$

where η represents the elevation and $A = \partial_x C/\sqrt{g}$ and $B = \sqrt{g}C^{-1}$ are pseudo-differential operators with the symbol of C given by $\hat{C}(k) = \Omega(k)/k$. The AB

equation can be interpreted as a higher order KdV equation for wave above finite depth and in certain approximation it becomes the KdV equation, see [3].

3. Third Order Asymptotic Approximations

In this section we present in some detail the results for the 3rd-order asymptotic solutions of the AB-equation, and we show for a few essential coefficients the difference in the coefficients when using the KdV equation.

3.1. Third order AB approximations

The solution of AB equation will be found by using a 3rd-order asymptotic method. For that aim the elevation η is expanded as power series; since we will restrict to 3rd-order, it is given by

$$\eta \approx \varepsilon\eta^{(1)} + \varepsilon^2\eta^{(2)} + \varepsilon^3\eta^{(3)}, \tag{3}$$

where $\eta^{(1)}$, $\eta^{(2)}$, $\eta^{(3)}$ represent the 1st, 2nd- and 3rd-order solution. Inserting this expansion in the AB equation, will give the following three linear partial differential equations that determine successively the three order contributions:

$$\partial_t\eta^{(1)} + \sqrt{g}A\eta^{(1)} = 0 \tag{4}$$

$$\partial_t\eta^{(2)} + \sqrt{g}A\eta^{(2)} = -\sqrt{g}A\left[\frac{1}{2}A(\eta^{(1)}A\eta^{(1)}) - \frac{1}{4}(A\eta^{(1)})^2 + \frac{1}{2}B(\eta^{(1)}B\eta^{(1)}) + \frac{1}{4}(B\eta^{(1)})^2\right] \tag{5}$$

$$\partial_t\eta^{(3)} + \sqrt{g}A\eta^{(3)} = -\sqrt{g}A\left[\frac{1}{2}A(\eta^{(1)}A\eta^{(2)} + \eta^{(2)}A\eta^{(1)}) - \frac{1}{4}(2A\eta^{(1)}A\eta^{(2)}) + \frac{1}{4}(2B\eta^{(1)}B\eta^{(2)}) + \frac{1}{2}B(\eta^{(1)}B\eta^{(2)} + \eta^{(2)}B\eta^{(1)})\right]. \tag{6}$$

In this paper, we choose for the solution of the first order equation (4) a bi-chromatic wave. This is defined as the sum of two monochromatic waves with the same amplitudes but different frequencies, $\omega_{\pm}$ and wave numbers $k_{\pm}$. Then

$$\eta^{(1)} = ae^{i\theta_+} + ae^{i\theta_-} + c.c, \tag{7}$$

where a is the amplitude, $\theta_\pm = k_\pm x - \omega_\pm t$ are the phases, $i = \sqrt{-1}$ is the complex unit and $c.c$ means conjugate complex. The dispersion relation $\omega_\pm = \Omega(k_\pm)$ is obtained by substituting this Ansatz to the first order equation. The 2nd-order contribution $\eta^{(2)}$ is obtained by solving (5). As a consequence of the quadratic nonlinearity, a resonance term will appear in the 3rd-order solution. This resonant contribution has to be made to vanish in order to satisfy the solvability condition for an asymptotically valid solution. To achieve this, we need to correct the wave number according to the Linstead Poincare method (6). Hence the wave number k is expanded in a power series like

$$k_\pm = k_\pm^{(0)} + \varepsilon k_\pm^{(1)} + \varepsilon^2 k_\pm^{(2)} + \cdots.$$

Using Taylor expansion of the symbols $\hat{A}$, $\hat{B}$ and $\hat{C}$ of the pseudo-differential operators A, B and C around $k_\pm^{(0)}$ to 2nd-order, we get $k_\pm^{(1)} = 0$, and the 2nd-order equation (5) becomes

$$\partial_t \eta^{(2)} + \sqrt{g} A \eta^{(2)} = RHS_1.$$

Here RHS_1 is the interaction of the first order solution with itself given by

$$RHS_1 = \alpha_{21} e^{2i\theta_+} + \alpha_{22} e^{2i\theta_-} + \alpha_{23} e^{i(\theta_+ + \theta_-)} + \alpha_{24} e^{i(\theta_+ - \theta_-)} + c.c.$$

The solution of the 2nd-order is chosen to be of the form

$$\eta^{(2)} = a_{21} e^{2i\theta_+} + a_{22} e^{2i\theta_-} + a_{23} e^{i(\theta_+ + \theta_-)} + a_{24} e^{i(\theta_+ - \theta_-)} + c.c. \tag{8}$$

Substituting $\eta^{(2)}$ into the 2nd-order equation, we find the coefficients of the 2nd-order solution as given below

$$a_{21} = \frac{\alpha_{21}}{\sqrt{g}\hat{A}(2k_+^{(0)}) - 2i\omega_+}; \quad a_{22} = \frac{\alpha_{22}}{\sqrt{g}\hat{A}(2k_-^{(0)}) - 2i\omega_-},$$

$$a_{23} = \frac{\alpha_{23}}{\sqrt{g}\hat{A}(k_+^{(0)} + k_-^{(0)}) - i(\omega_+ + \omega_-)}; \; a_{24} = \frac{\alpha_{24}}{\sqrt{g}\hat{A}(k_+^{(0)} + k_-^{(0)}) - i(\omega_+ - \omega_-)};$$

the expressions for α_{21}, ..., α_{24} are given in the Annex.

The wave number correction $k_{\pm}^{(2)}$ is found from the 3rd-order equation when removing the resonance terms. These wave numbers result from the interaction of the 1st- and 2nd-order terms and are given by

$$k_{+}^{(2)} = \frac{\alpha_{37}}{ia(k_{+}^{(0)}\hat{C}'(k_{+}^{(0)}) + \hat{C}(k_{+}^{(0)}))}; \quad k_{-}^{(2)} = \frac{\alpha_{38}}{ia(k_{-}^{(0)}\hat{C}'(k_{-}^{(0)}) + \hat{C}(k_{-}^{(0)}))}.$$

The 3rd-order equation then becomes

$$\partial_t \eta^{(3)} + \sqrt{g} A \eta^{(3)} = RHS_2,$$

where RHS_2 is given by

$$RHS_2 = \alpha_{31} e^{3i\theta_+} + \alpha_{32} e^{3i\theta_-} + \alpha_{33} e^{i(2\theta_+ + \theta_-)} + \alpha_{34} e^{i(2\theta_- + \theta_+)} + \alpha_{35} e^{i(2\theta_+ - \theta_-)} + \alpha_{36} e^{i(2\theta_- - \theta_+)} + c.c,$$

and $\alpha_{31}, ..., \alpha_{38}$ are detailed in the Annex. The 3rd-order contribution to the solution is taken as

$$\eta^{(3)} = \alpha_{31} e^{3i\theta_+} + \alpha_{32} e^{3i\theta_-} + \alpha_{33} e^{i(2\theta_+ + \theta_-)} + \alpha_{34} e^{i(2\theta_- + \theta_+)} + a_{35} e^{i(2\theta_+ - \theta_-)} + a_{36} e^{i(2\theta_- - \theta_+)} + c.c. \tag{9}$$

Substituted into the 3rd-order equation, we find the coefficients as given below:

$$a_{31} = \frac{\alpha_{31}}{-3i\omega_+ + \sqrt{g}\hat{A}(3k_{+}^{(0)})}; \; a_{32} = \frac{\alpha_{32}}{-3i\omega_- + \sqrt{g}\hat{A}(3k_{-}^{(0)})};$$

$$a_{33} = \frac{\alpha_{33}}{-i(2\omega_+ + \omega_-) + \sqrt{g}\hat{A}(2k_{+}^{(0)} + k_{-}^{(0)})};$$

$$a_{34} = \frac{\alpha_{34}}{-i(2\omega_- + \omega_+) + \sqrt{g}\hat{A}(2k_{-}^{(0)} + k_{+}^{(0)})};$$

$$a_{35} = \frac{\alpha_{35}}{-i(2\omega_+ + \omega_-) + \sqrt{g}\hat{A}(2k_{+}^{(0)} + k_{-}^{(0)})};$$

$$a_{36} = \frac{\alpha_{34}}{-i(2\omega_- - \omega_+) + \sqrt{g}\hat{A}(2k_{-}^{(0)} - k_{+}^{(0)})}.$$

The second and 3rd-order contributions are called bound waves because these are intimately connected to the 1st-order solution since they have same velocity. Particularly in the 3rd-order solution, the bound waves contain side-band waves and non side-band waves. The side-band waves have frequencies determined by the signal input given by $2\omega_+ - \omega_-$ and $2\omega_- - \omega_+$. The non side-band waves have larger frequencies. Cahyono in [2], has shown that the side-band waves of 3rd-order are of large influence since they can be of the same order as the 1st-order solution. This can be understood since the order of the side band waves is given by $a\left(\frac{a}{\kappa}\right)^2$; hence for sufficiently small κ, i.e., sufficiently large modulation length of the bi-chromatic, a/κ will be of order unity. The other 3rd-order terms are much smaller than the 2nd-order terms and will be neglected in the following.

The bound waves of the 2nd- and 3rd-order solution will give a contribution to the signal at the wave maker. Hence, if we want to prescribe the bi-chromatic wave as input signal, the bound waves should be compensated by 2nd- and 3rd- order free waves, written as $\eta_{fw}^{(2)}$ and $\eta_{fw}^{(3)}$ respectively. These free waves have the same frequencies as the bound waves but satisfy the exact dispersion relation.

Summarizing the result, we write the approximate solution of the AB equation from 3rd-order asymptotic method as

$$\eta = \eta^{(1)} + \eta_{bw}^{(2)} - \eta_{fw}^{(2)} + \eta_{bw}^{(3)} - \eta_{fw}^{(3)}.$$

In Figure 1 we illustrate the nonlinear 2nd- and 3rd-order mode generation.

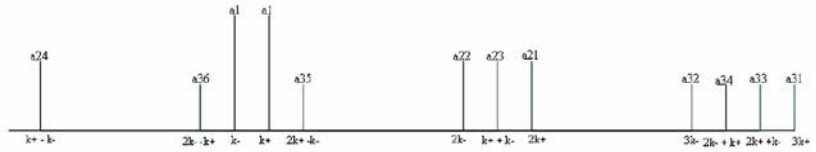

Figure 1. Nonlinear mode generation in second and third order from the two basic wave numbers in the bi-chromatic wave.

3.2. Comparison with KdV approximations

Using the KdV-equation instead of the AB-equation, a similar 3rd-order approximation can be derived. The difference of the 3rd-order AB- and KdV-

approximations can be illustrated by giving the differences in some of the main coefficients. Using obvious notation, we have in 2nd-order

$$(a_{21})_{AB} = \beta(k_+^{(0)})(a_{21})_{KdV} \tag{10}$$

with

$$(a_{21})_{KdV} = \frac{3a^2 k_+^{(0)}}{2(2\omega_+ - \Omega(2k_+^{(0)}))},$$

$$\beta(k_+^{(0)}) = \frac{1}{3}(k_+^{(0)})^2 \hat{C}^2(k_+^{(0)})\hat{C}(2k_+^{(0)}) - \frac{4}{3}(k_+^{(0)})^2 \hat{C}^2(2k_+^{(0)})\hat{C}(k_+^{(0)})$$

$$+ \frac{1}{3}\frac{\hat{C}(2k_+^{(0)})}{\hat{C}^2(k_+^{(0)})} + \frac{2}{3}\frac{\hat{C}(2k_+^{(0)})}{\hat{C}(k_+^{(0)})\hat{C}(2k_+^{(0)})}.$$

For 3rd-order, we get for instance

$$(a_{31})_{AB} = \beta^*(k_+^{(0)})(a_{31})_{KdV}, \tag{11}$$

with

$$(a_{31})_{KdV} = \frac{9a\, a_{21} k_+^{(0)}}{2(3\omega_+ - \Omega(3k_+^{(0)}))},$$

$$\beta^*(k_+^{(0)}) = \frac{2}{3}(k_+^{(0)})^2 \hat{C}(k_+^{(0)})\hat{C}(2k_+^{(0)})\hat{C}(3k_+^{(0)}) - (k_+^{(0)})^2[\hat{C}(k_+^{(0)})$$

$$+ 2\hat{C}(2k_+^{(0)})]\hat{C}^2(3k_+^{(0)}) + \frac{1}{3}\frac{\hat{C}(3k_+^{(0)})}{\hat{C}(k_+^{(0)})\hat{C}(2k_+^{(0)})}$$

$$+ \frac{1}{3}\left[\frac{1}{\hat{C}(k_+^{(0)})} + \frac{1}{\hat{C}(2k_+^{(0)})}\right].$$

Graphically, the coefficients are plotted as function of wave number in Figures 2 and 3. Although the asymptotic values for long waves coincide, as expected, the difference in these coefficients will lead to noticeable effects in the approximations as will be shown in the next section.

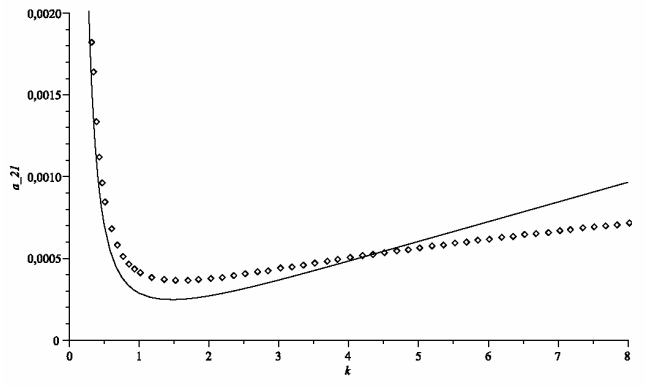

Figure 2. The coefficients of second order a_{21} for AB (line) and KdV (point).

4. Comparisons of Bi-chromatic Evolutions

In this section we compare numerical simulations of the AB-equation with measurements of experiments in a wave tank of 200m long of MARIN hydrodynamic laboratory. The good agreement makes it possible to consider the AB-simulations as producing the correct waves for which then the maximal position and amplitudes can be detected. Time signals at certain locations in the wave tank will be determined by the AB-simulations and by the 3rd-order approximations using the AB- and the KdV-equation. The numerically computed MTA will be compared with the MTA as calculated with the two 3rd-order approximations. In the final subsection we will give explicit expressions for the maximal position and amplitude amplification.

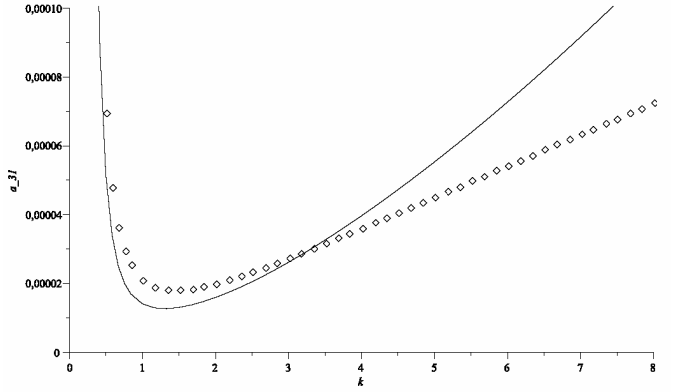

Figure 3. The coefficients of third order a_{31} of AB (line) and KdV (point).

4.1. Numerical simulations compared with experiments

Numerical simulation with the AB-equation were reported in [4] using a high order pseudo-spectral implementation, using 1024*3 modes for calculations over more than 150 wave lengths, in a time period of 400s and over a spatial interval of 800m length. Here we will show some results. As input at $x = 10m$ (downstream of the waveflap) is taken the signal from the bi-chromatic wave experiment at the laboratory. In Figure 4 we show the comparison between the numerical calculation and the MARIN data: at the left the measured time signals and at the right the corresponding signals calculated with the AB equation, for various locations. Observe the good agreement, illustrating that the AB-simulation captures well the substantial envelope deformations.

4.2. Third order approximations

In this subsection we discuss the evolution of bi-chromatic wave using the 3rd-order asymptotic approximation for the AB- and KdV-equation. We will compare the results with each other and with numerical AB-simulations. We take as input signal at $x = 0m$ the expression

$$\eta(0, t) = 4a \cos(\overline{\omega} t) \cos(\nu t), \tag{12}$$

where a is the amplitude, and $\overline{\omega} = \frac{1}{2}(\omega_+ + \omega_+)$ and $\nu = \frac{1}{2}(\omega_+ - \omega_+)$ are the carrier frequency and the modulation frequency respectively.

The details of the approximation of the AB- and the KdV-equation for parameter of $a = 0.5m$, $\overline{\omega} = 3.1495[1/s]$ and $\nu = 0.1575[1/s]$ at position of $x = 40m$ can be seen in Figures 5 and 6. The contributions of the 2nd-order terms are almost identical, but in 3rd-order the AB-contribution differs substantially from KdV, being roughly twice as large. This is a consequence of the difference of the nonlinear terms in the equations. The wave signals for the parameters at several positions are shown in Figure 7, with the 3rd-order KdV- and AB-approximation at the left and at the right respectively, and the numerical AB-calculation in the middle.

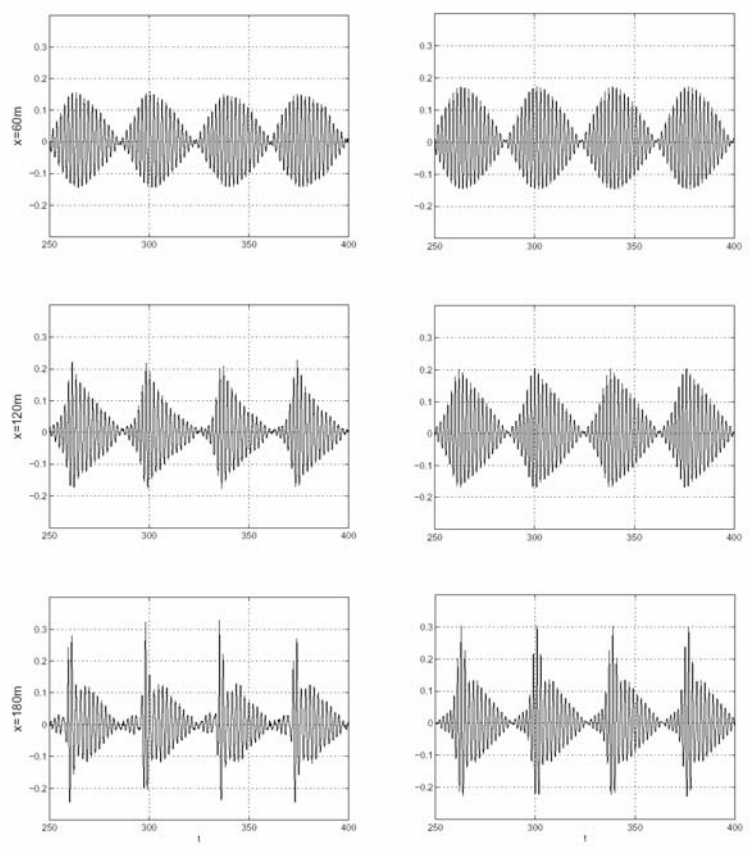

Figure 4. The bi-chromatic wave signal which is captured as time signals at positions $x = 60m,\ 120m, 180m$, at the left for the MARIN experiment and at the right as simulated with the AB-equation.

Qualitatively it seems that the performance of the 3rd-order asymptotic approximation with AB resembles the numerical simulation closer than the 3rd-order KdV-approximation. However, for larger distances from the input position, the shape of the signal of both approximations deviates more from the actual evolution represented by the numerical solution. This is mainly caused by the fact that both AB- and KdV-approximations retain the initial symmetry in each beat pattern that is lost in the actual evolution. Except this, the AB-approximation has higher and more accurate amplitude than the KdV-approximation. Observe also that both approximations are quite well capable to predict the propagation speed, as is seen from the positioning of the beats; this is a consequence of the exact linear dispersion

(for both approximations) and the limited influence of the difference in the 2nd-order wave number corrections.

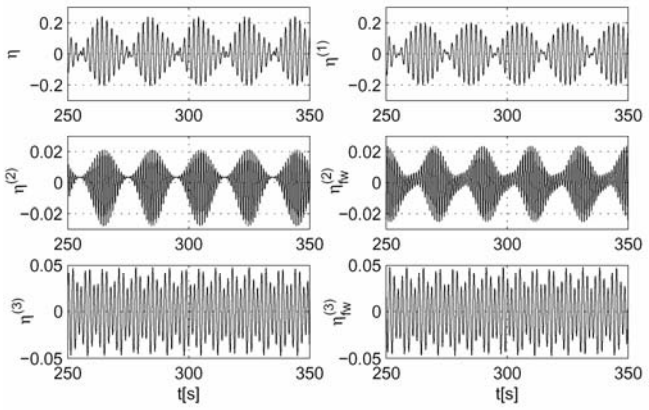

Figure 5. The solution of AB equation, η, $\eta^{(1)}$, $\eta^{(2)}$, $\eta^{(2)}_{fw}$, $\eta^{(3)}$, $\eta^{(3)}_{fw}$ represent the total, first order, second order, second order free wave, third order and third order free wave solution respectively.

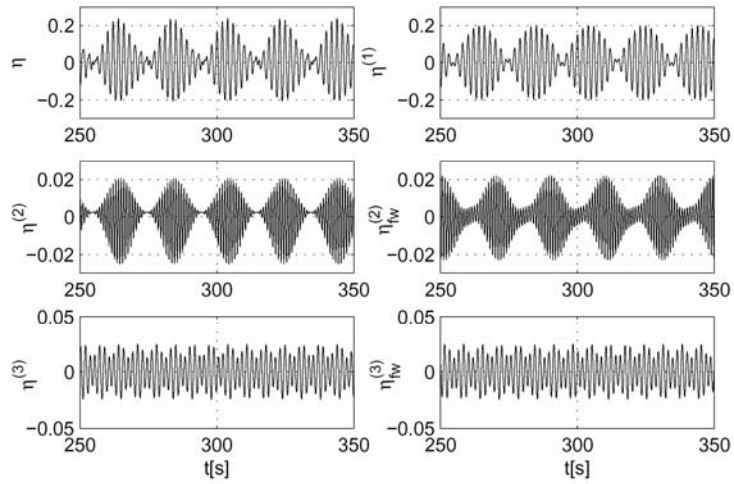

Figure 6. The solution of KdV equation, η, $\eta^{(1)}$, $\eta^{(2)}$, $\eta^{(2)}_{fw}$, $\eta^{(3)}$, $\eta^{(3)}_{fw}$ represent the total, first order, second order, second order free wave, third order and third order free wave solution respectively.

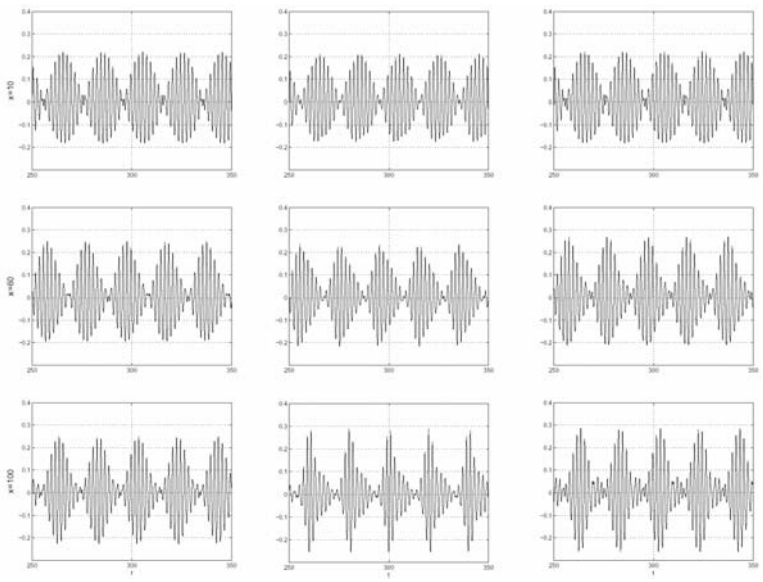

Figure 7. The bi-chromatic signals computed with third order asymptotic of KdV (left) and numerical simulation of AB (mid) and third order asymptotic of AB(right) at $x = 10,\ 60,\ 100$m.

4.3. MTA calculations

The profiles approximated with the 3rd-order calculations do not yet given an indication about the quality to predict the global evolution, such as the location of the largest wave height in the tank $(x_{\max})$ and how large the amplitude amplification is. In order to investigate this further, we will consider the graph of the so-called maximal temporal amplitude (MTA), which is defined as

$$\mathcal{M}(x) = \max_{t \in [0,\ T]} \eta(x,\ t),$$

where $\eta(x,\ t)$ is the elevation and $[0,\ T]$ is the observation time interval. The MTA will give an abstracted view of the global evolution and can be used to determine the position $x_{\max}$ of maximal wave height in the tank and the ratio of this maximal height with the initial amplitude, the so-called Amplitude Amplification (AA). For experimental data, that are captured in a few positions only, the MTA cannot be determined. We will use the MTA to compare the three model results: the MTA as found from the numerical AB-simulation, and from the 3rd-order approximations

with AB and KdV. As example we present these results in Figure 8 for the bi-chromatic wave group with parameters $a = 0.05m$, $\overline{\omega} = 3.1495[1/s]$ and $\nu = 0.1575[1/s]$.

First we comment on the general shape of the displayed MTA's. These plots are obtained for a simulation time interval with $T = 400[s]$. From the 3rd-order solution it is clear that the short oscillation is due to the 2nd-order contribution. However, the oscillation period is different than the period of the 2nd-order solution, because in the numerics the contribution of many higher order waves is included. In Figure 9 we plotted for some cases the MTA of the 3rd-order approximation with and without the 2nd-order contributions, in the left and right plot respectively.

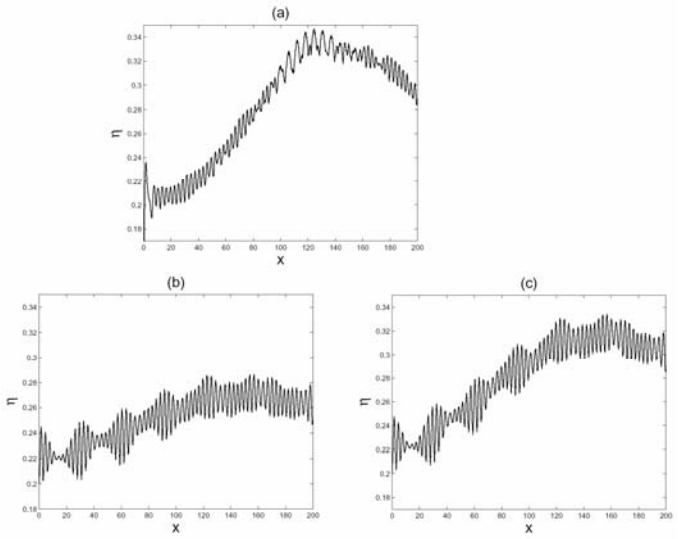

Figure 8. MTA curve using numerical calculation of AB (a), third order asymptotic of KdV (b) and third order asymptotic of AB (c).

This leads to the conclusion that if we want to obtain the MTA with 3rd-order approximation, we will have

$$\mathcal{M}^{(3)}(x) = \max_{t\in[0,T]} \eta(x, t) \tag{13}$$

$$\approx \max_{t\in[0,T]} [\eta(x, t) - 2^{nd} - \text{order}(t)] + 2^{nd} \text{-order wave height.} \tag{14}$$

This has to be taken into account when we want to calculate the MTA with the 3rd-order approximation in the next subsection.

We will now comment on the differences between the MTA's obtained from the different approximations. The MTA of 3rd-order approximation with the AB-equation is closer to the MTA of the numerical calculation than the MTA of 3rd-order approximation with the KdV-equation. The maximum amplitude for these cases are $0.347m$, $0.335m$, $0.28m$ for the numerical AB-simulation, the 3rd-order AB and 3rd-order KdV approximation respectively; the maximal position is in the range of $120m - 130m$.

4.4. MTA dependence on wave parameters

The MTA shows the maximal wave heights over the spatial interval of interest. Hence we can find the maximal position and the amplification factor. To get the results, we use the MTA(3) for the 3rd order approximations. The 3rd-order approximation makes it possible to give an explicit formula for the position of maximal wave height (in a given spatial interval). This has been done for the KdV-approximation in [5].

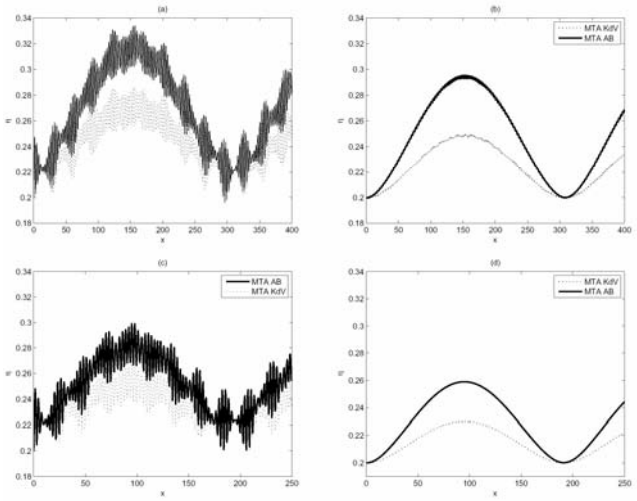

Figure 9. MTA curve for different parameter ν, (a) $\nu = 0.1575[1/s]$ (c) $\nu = 0.2[1/s]$ with second order solution and (b) $\nu = 0.1575[1/s]$ (d) $\nu = 0.2[1/s]$ without second order solution for AB (continues line) and KdV (dot line), for amplitude $a = 0.05[m]$ and frequency $\overline{\omega} = 3.1495[1/s]$.

Using the AB 3th-order approximation, these quantities are given explicitly by

$$x_{\max} \approx \frac{\pi}{|\,\overline{K} - k\,|}, \tag{15}$$

Where $\overline{K} = \dfrac{\Omega^{-1}(\overline{\omega} + 3\nu) + \Omega^{-1}(\overline{\omega} - 3\nu)}{2}$ and $\overline{k} = \dfrac{k_+ + k_-}{2}$.

Note that for $x_{\max}$ we only have to consider the 1st- and 3th-order terms, while for the amplitude amplification we added the 2nd-order contribution to the 1st-and 3th-order terms. From the expressions it is clear that both quantities depend in a complicated way on the parameters of the Bi-chromatic, i.e. on the initial amplitude a, the carrier frequency $\overline{\omega}$ and the modulation frequency ν.

We will now present in a graphical way the dependence of $x_{\max}$ and the amplitude amplification (AA) on the parameters, and compare the analytic results of the 3th-order approximation of AB with of the 3th-order approximation of KdV. These results are given in Figure 10. The results show that an increase of amplitude, carrier-frequency or envelope-frequency decreases the distance of $x_{\max}$ to the wave maker. An increase of amplitude and carrier-frequency or a decrease of envelope-frequency increases the AA. The effect of the envelope-frequency on the amplification is mostly caused by the 3th-order contribution that is of the order $\mathcal{O}\left(a\left(\dfrac{a}{\nu}\right)^2\right)$.

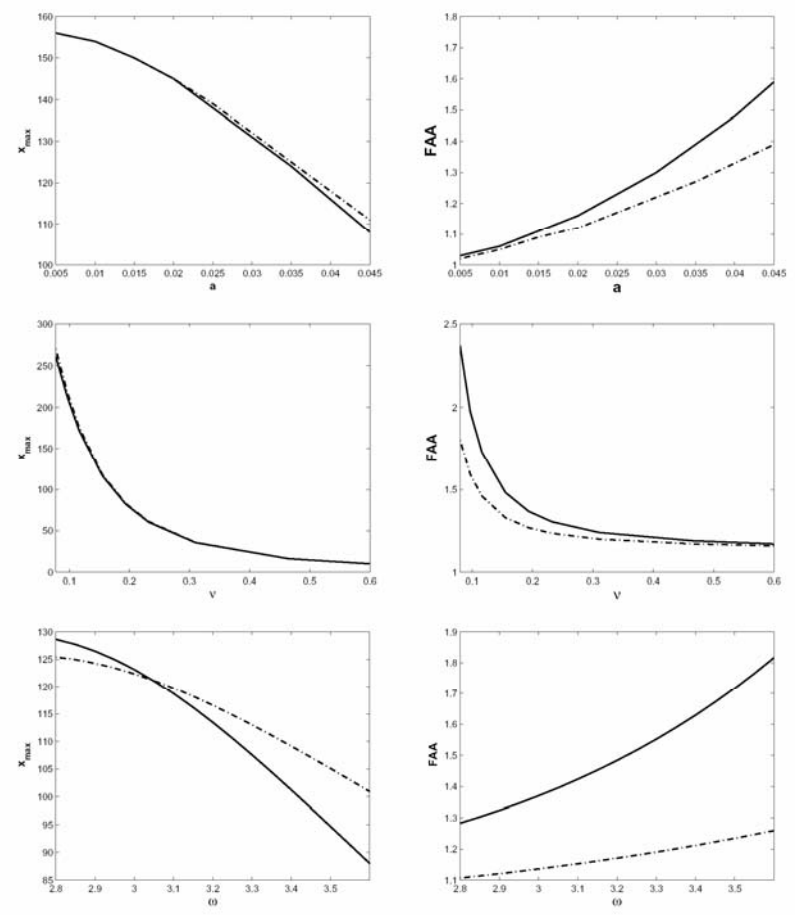

Figure 10. The dependence of the position of maximal amplitude (left) and Amplitude Amplification (right) on amplitude, frequency of carrier and frequency of envelope, for some $a = 04m$, $\overline{\omega} = 3.145[1/s]$ and $\nu = 0.155[1/s]$ for AB (line) and KdV (dash line)

5. Conclusions and Remarks

In this paper we studied the nonlinear deformation of bi-chromatic wave groups. The propagation of the wave groups was shown to be well captured by numerical simulations with the AB-equation, and we used these simulations to compare with results of explicit 3th-order approximations. For these 3th-order approximations we used two model equations: the AB-equation that was used for the numerical

simulations and a KdV-equation which has exact linear dispersion (just like AB) but has as nonlinear terms those of the classical KdV equation. Note that the AB-equation includes dispersion in the nonlinear terms so that it is exact in second order. We argued and showed that the details of the wave group distortion are dominated by the resonant 3th-order terms, which are actually of the order $\mathcal{O}\left(a\left(\frac{a}{\nu}\right)^2\right)$, where ν is the modulation frequency. Since the 3th-order terms in the 3th-order approximation are determined by the 1st- and 2nd-order terms, the better nonlinear quality of the AB-equation will lead to better results in 2nd, and therefore also in 3th-order terms when compared to the corresponding KdV terms. This could clearly be shown by comparison with the numerical AB-simulation.

The time-signal at observation positions in the down stream direction is somewhat better for AB 3th-order than the KdV 3th-order approximation. But the prediction of the maximal position and amplitude amplification is remarkably well predicted by the explicit formulas from the AB 3th-order approximation, as was shown in Figure. 8. The somewhat lower values of AA can be understood since higher than 3rd-order contributions are needed to achieve a larger wave height. The explicit formulas give a simple tool for applications in hydrodynamic laboratories where high waves are desired at a pre-determined position in the tank. In this way the nonlinear effects in the bi-chromatic wave group can be exploited in a deterministic way to produce waves of much higher amplitude than could be generated by the wave flap in the absence of nonlinear effects.

Acknowledgments

The authors wish to thank Prof. E. (Brenny) van Groesen for many rewarding discussions and for his constant support for the research. The numerical simulations were performed for the major part while the first author was visiting the University of Twente as PhD-sandwich funded by the Indonesian Ministry of Education (DIKTI). This research is part of an Incentive Research Grant 2008 from the Indonesian Minister of Research and Technology.

References

[1] Andonowati, E. van Groesen, Optical pulse deformation in 2nd-order nonlinear media, Journal of Nonlinear Optics Physics and Materials 12 (2003), 221-234.

[2] E. Cahyono, Analytical wave codes for predicting surface waves in a laboratory basin, Ph. D Thesis, Fac. of Mathematical Sciences Univ. of Twente, The Nether-lands, 2002.

[3] E. van Groesen, Andonowati, Variational derivation of KdV-type of models for surface water waves, Physics Letters A 366 (2007), 195-201.

[4] E. van Groesen, Andonowati, L. She Lia, I. Lakhturov, Accurate modelling of unidirectional surface waves, J. Comput. Appl. Math. 234 (2009), 1747-1756.

[5] Marwan, Surface water waves: theory, numerics, and its applications on the generation of extreme waves, PhD thesis, Institut Teknologi Bandung, 2006.

[6] C. T. Stanberg, On the non-linear behaviour of ocean wave gorups, In: B. L. Edgeand J. M. Hemsley (eds), Ocean Wave Measurement and Analysis, Reston, VA, USA: American Society of Civil Engineers (ASCE) 2 (1998), 1227-1241.

[7] J. Westhuis, E. van Groesen, R. H. M. Huijsmans, Experiments and numerics of bichromatic wave groups, J. Waterway, Port, Coastal and Ocean Engineering, 127 (2001), 334-342.

Annex

I. The coefficients in the 2nd -order solution of AB

$$\alpha_{21} = -\sqrt{g}a^2\Big[-\frac{1}{4}\hat{A}^2(k_+^{(0)})\hat{A}(2k_+^{(0)}) + \frac{1}{2}\hat{A}^2(k_+^{(0)})\hat{A}^2(2k_+^{(0)}) + \frac{1}{4}\hat{B}^2(k_+^{(0)})\hat{A}(2k_+^{(0)})$$

$$\frac{1}{2}\hat{B}(k_+^{(0)})\hat{B}(2k_+^{(0)})\hat{A}(2k_+^{(0)})\Big].$$

$$\alpha_{22} = -\sqrt{g}a^2\Big[-\frac{1}{4}\hat{A}^2(k_-^{(0)})\hat{A}(2k_-^{(0)}) + \frac{1}{2}\hat{A}^2(k_-^{(0)})\hat{A}^2(2k_-^{(0)}) + \frac{1}{4}\hat{B}^2(k_-^{(0)})\hat{A}(2k_-^{(0)})$$

$$\frac{1}{2}\hat{B}(k_-^{(0)})\hat{B}(2k_-^{(0)})\hat{A}(2k_-^{(0)})\Big].$$

$$\alpha_{23} = -\sqrt{g}a^2\Big[-\frac{1}{2}\hat{A}^2(k_+^{(0)})\hat{A}(k_-^{(0)})\hat{A}(k_+^{(0)}+k_-^{(0)}) + \frac{1}{2}(\hat{A}(k_+^{(0)})$$

$$+ \hat{A}(k_-^{(0)}))\hat{A}(k_+^{(0)}+k_-^{(0)})$$

$$+ \frac{1}{2}\hat{B}(k_+^{(0)})\hat{B}(k_-^{(0)})\hat{A}(k_+^{(0)}+k_-^{(0)}) + \frac{1}{2}(\hat{B}(k_+^{(0)}) + \hat{B}(k_-^{(0)}))\hat{B}(k_+^{(0)}+k_-^{0})$$

$$\hat{A}(k_+^{(0)}+k_-^{(0)})\Big].$$

$$\alpha_{24} = -\sqrt{g}a^2\Big[-\frac{1}{2}\hat{A}^2(k_+^{(0)})\hat{A}(k_-^{(0)})\hat{A}(k_+^{(0)}+k_-^{(0)})$$

$$+\frac{1}{2}(\hat{A}(k_+^{(0)})-\hat{A}(k_-^{(0)}))\hat{A}^2(k_+^{(0)}+k_-^{(0)})$$

$$+\frac{1}{2}\hat{B}(k_+^{(0)})\hat{B}(k_-^{(0)})\hat{A}(k_+^{(0)}+k_-^{(0)})+\frac{1}{2}(\hat{B}(k_+^{(0)})+\hat{B}(k_-^{(0)}))\hat{B}(k_+^{(0)}-k_-^{0})$$

$$\hat{A}(k_+^{(0)}+k_-^{(0)})\Big].$$

II. The coefficients in the 3rd-order solution of AB

$$\alpha_{31} = -\sqrt{g}\Big[-\frac{1}{2}aa_{21}\hat{A}(k_+^{(0)})\hat{A}(2k_+^{(0)})+\frac{1}{2}aa_{21}(\hat{A}(k_+^{(0)})+\hat{A}(2k_+^{(0)}))\hat{A}(3k_+^{(0)})$$

$$+\frac{1}{2}aa_{21}\hat{B}(k_+^{(0)})\hat{B}(2k_+^{(0)})+\frac{1}{2}aa_{21}(\hat{B}(k_+^{(0)})+\hat{B}(2k_+^{(0)}))\hat{B}(3k_+^{(0)})\Big]\hat{A}(3k_+^{(0)})e^{3i\theta_+}.$$

$$\alpha_{32} = -\sqrt{g}\Big[-\frac{1}{2}aa_{22}\hat{A}(k_-^{(0)})\hat{A}(2k_-^{(0)})+\frac{1}{2}aa_{22}(\hat{A}(k_-^{(0)})+\hat{A}(2k_-^{(0)}))\hat{A}(3k_-^{(0)})$$

$$+\frac{1}{2}aa_{22}\hat{B}(k_-^{(0)})\hat{B}(2k_-^{(0)})+\frac{1}{2}aa_{22}(\hat{B}(k_-^{(0)})+\hat{B}(2k_-^{(0)}))\hat{B}(3k_-^{(0)})\Big]\hat{A}(3k_-^{(0)})e^{3i\theta_-}.$$

$$\alpha_{33} = -\sqrt{g}\Big[-\frac{1}{2}aa_{23}\hat{A}(k_+^{(0)})\hat{A}(k_+^{(0)}+k_-^{(0)})-\frac{1}{2}aa_{21}\hat{A}(k_-^{(0)})\hat{A}(2k_+^{(0)})$$

$$+\Big[\frac{1}{2}aa_{23}(\hat{A}(k_+^{(0)})+\hat{A}(k_+^{(0)}+k_-^{(0)}))+\frac{1}{2}aa_{21}(\hat{A}(k_-^{(0)})+\hat{A}(2k_+^{(0)}))\Big]\hat{A}(k_-^{(0)}+2k_+^{(0)})$$

$$+\frac{1}{2}aa_{23}\hat{B}(k_+^{(0)})\hat{B}(k_+^{(0)}+k_-^{(0)})-\frac{1}{2}aa_{21}\hat{B}(k_-^{(0)})\hat{B}(2k_+^{(0)})$$

$$+\Big[\frac{1}{2}aa_{23}(\hat{B}(k_+^{(0)})+\hat{B}(k_+^{(0)}+k_-^{(0)}))+\frac{1}{2}aa_{22}(\hat{B}(k_-^{(0)})+\hat{B}(2k_+^{(0)}))\Big]$$

$$\hat{B}(k_-^{(0)}+2k_+^{(0)})\Big]\hat{A}(k_-^{(0)}+2k_+^{(0)})e^{i(2\theta_++\theta_-)}.$$

$$\alpha_{34} = -\sqrt{g}\Big[-\frac{1}{2}aa_{23}\hat{A}(k_-^{(0)})\hat{A}(k_+^{(0)}+k_-^{(0)})-\frac{1}{2}aa_{22}\hat{A}(k_+^{(0)})\hat{A}(2k_-^{(0)})$$

$$+\Big[\frac{1}{2}aa_{23}(\hat{A}(k_-^{(0)})+\hat{A}(k_+^{(0)}+k_-^{(0)}))+\frac{1}{2}aa_{22}(\hat{A}(k_+^{(0)})+\hat{A}(2k_-^{(0)}))\Big]$$

$$\hat{A}(k_+^{(0)}+2k_-^{(0)})+\frac{1}{2}aa_{23}\hat{B}(k_-^{(0)})\hat{B}(k_+^{(0)}+k_-^{(0)})-\frac{1}{2}aa_{22}\hat{B}(k_+^{(0)})\hat{B}(2k_-^{(0)})$$

$$+\left[\frac{1}{2}aa_{23}(\hat{B}(k_-^{(0)})+\hat{B}(k_+^{(0)}+k_-^{(0)}))+\frac{1}{2}aa_{22}(\hat{B}(k_+^{(0)})+\hat{B}(2k_-^{(0)}))\right]$$

$$\hat{B}(k_+^{(0)}+2k_-^{(0)})\Big]\hat{A}(k_+^{(0)}+2k_-^{(0)})e^{i(2\theta_-+\theta_+)}.$$

$$\alpha_{35}=-\sqrt{g}\Big[-\frac{1}{2}aa_{24}\hat{A}(k_+^{(0)})\hat{A}(k_+^{(0)}-k_-^{(0)})+\frac{1}{2}aa_{21}\hat{A}(k_-^{(0)})\hat{A}(2k_+^{(0)})$$

$$+\left[\frac{1}{2}aa_{24}(\hat{A}(k_+^{(0)})+\hat{A}(k_+^{(0)}+k_-^{(0)}))+\frac{1}{2}aa_{21}(\hat{A}(2k_+^{(0)})-\hat{A}(k_-^{(0)}))\right]$$

$$\hat{A}(2k_+^{(0)}-k_-^{(0)})+\frac{1}{2}aa_{24}\hat{B}(k_+^{(0)})\hat{B}(k_+^{(0)}-k_-^{(0)})+\frac{1}{2}aa_{21}\hat{B}(k_-^{(0)})\hat{B}(2k_+^{(0)})$$

$$+\left[\frac{1}{2}aa_{24}(\hat{B}(k_+^{(0)})+\hat{B}(k_+^{(0)}-k_-^{(0)}))+\frac{1}{2}aa_{21}(\hat{B}(2k_+^{(0)})+\hat{B}(k_-^{(0)}))\right]$$

$$\hat{B}(2k_+^{(0)}-k_-^{(0)})\Big]\hat{A}(2k_+^{(0)}-k_-^{(0)})e^{i(2\theta_+-\theta_-)}.$$

$$\alpha_{36}=-\sqrt{g}\Big[\frac{1}{2}aa_{24}\hat{A}(k_-^{(0)})\hat{A}(k_+^{(0)}-k_-^{(0)})+\frac{1}{2}aa_{22}\hat{A}(k_+^{(0)})\hat{A}(2k_-^{(0)})$$

$$+\left[\frac{1}{2}aa_{24}(\hat{A}(k_-^{(0)})-\hat{A}(k_+^{(0)}-k_-^{(0)}))+\frac{1}{2}aa_{22}(\hat{A}(2k_-^{(0)})-\hat{A}(k_+^{(0)}))\right]$$

$$\hat{A}(2k_-^{(0)}-k_+^{(0)})+\frac{1}{2}aa_{24}\hat{B}(k_-^{(0)})\hat{B}(k_+^{(0)}-k_-^{(0)})+\frac{1}{2}aa_{22}\hat{B}(k_+^{(0)})\hat{B}(2k_-^{(0)})$$

$$+\left[\frac{1}{2}aa_{24}(\hat{B}(k_-^{(0)})+\hat{B}(k_+^{(0)}-k_-^{(0)}))+\frac{1}{2}aa_{22}(\hat{B}(2k_-^{(0)})+\hat{B}(k_+^{(0)}))\right]$$

$$\hat{B}(2k_-^{(0)}-k_+^{(0)})\Big]\hat{A}(2k_-^{(0)}-k_+^{(0)})e^{i(2\theta_--\theta_+)}.$$

$$\alpha_{37}=-\sqrt{g}\Big[\frac{1}{2}aa_{21}\hat{A}(k_+^{(0)})\hat{A}(k_+^{(0)})-\frac{1}{2}aa_{24}\hat{A}(k_-^{(0)})\hat{A}(k_+^{(0)}-k_-^{(0)})$$

$$\frac{1}{2}aa_{23}\hat{A}(k_-^{(0)})\hat{A}(k_+^{(0)}+k_-^{(0)})+\Big[\frac{1}{2}aa_{21}(\hat{A}(2k_+^{(0)})-\hat{A}(k_+^{(0)}))$$

$$+\frac{1}{2}aa_{24}(\hat{A}(k_+^{(0)}-k_-^{(0)})+\hat{A}(k_-^{(0)}))+\frac{1}{2}aa_{23}(\hat{A}(k_+^{(0)}+k_-^{(0)})$$

$$-\hat{A}(k_-^{(0)}))\Big]\hat{A}(k_+^{(0)})+\frac{1}{2}aa_{21}\hat{B}(k_+^{(0)})\hat{B}(2k_+^{(0)})+\frac{1}{2}aa_{24}\hat{B}(k_-^{(0)})$$

$$\hat{B}(k_+^{(0)}-k_-^{(0)})+\frac{1}{2}aa_{23}\hat{B}(k_-^{(0)})\hat{B}(k_+^{(0)}+k_-^{(0)})+\Big[\frac{1}{2}aa_{21}(\hat{B}(2k_+^{(0)})$$

$$+\hat{B}(k_+^{(0)}))+\frac{1}{2}aa_{24}(\hat{B}(k_+^{(0)}-k_-^{(0)})+\hat{B}(k_-^{(0)}))$$

$$+\frac{1}{2}aa_{23}(\hat{B}(k_+^{(0)}+k_-^{(0)})+\hat{B}(k_-^{(0)}))\Big]\hat{B}(k_+^{(0)})\Big]\hat{A}(k_+^{(0)})e^{i\theta_+}.$$

$$\alpha_{38}=-\sqrt{g}\Big[\frac{1}{2}aa_{22}\hat{A}(k_-^{(0)})\hat{A}(2k_-^{(0)})+\frac{1}{2}aa_{24}\hat{A}(k_+^{(0)})\hat{A}(k_+^{(0)}-k_-^{(0)})$$

$$+\frac{1}{2}aa_{23}\hat{A}(k_+^{(0)})\hat{A}(k_+^{(0)}+k_-^{(0)})+\Big[\frac{1}{2}aa_{22}(\hat{A}(2k_-^{(0)})-\hat{A}(k_-^{(0)}))$$

$$+\frac{1}{2}aa_{24}(-\hat{A}(k_+^{(0)}-k_-^{(0)})+\hat{A}(k_+^{(0)}))+\frac{1}{2}aa_{23}(\hat{A}(k_+^{(0)}+k_-^{(0)})$$

$$-\hat{A}(k_+^{(0)}))\Big]\hat{A}(k_-^{(0)})+\frac{1}{2}aa_{22}\hat{B}(k_-^{(0)})\hat{B}(2k_-^{(0)})+\frac{1}{2}aa_{24}\hat{B}(k_+^{(0)})$$

$$\hat{B}(k_+^{(0)}-k_-^{(0)})+\frac{1}{2}aa_{23}\hat{B}(k_+^{(0)})\hat{B}(k_+^{(0)}+k_-^{(0)})+\Big[\frac{1}{2}aa_{22}(\hat{B}(2k_-^{(0)})$$

$$+\hat{B}(k_-^{(0)}))+\frac{1}{2}aa_{24}(\hat{B}(k_+^{(0)}-k_-^{(0)})+\hat{B}(k_+^{(0)}))$$

$$+\frac{1}{2}aa_{23}(\hat{B}(k_+^{(0)}+k_-^{(0)})+\hat{B}(k_+^{(0)}))\Big]\hat{B}(k_-^{(0)})\Big]\hat{A}(k_-^{(0)})e^{i\theta_-}.$$